Day-ahead trading of wind-battery hybrid power plants

Wind forecast uncertainty and limited feed-in grid connection

Ledro, Mirko; Vicari, Alessandro; Mouette, Gauthier; Sørensen, Jens Jakob; Zepter, Jan Martin; Marinelli, Mattia

Publication date:
2024

Document Version
Publisher's PDF, also known as Version of record

DAY-AHEAD TRADING OF WIND-BATTERY HYBRID POWER PLANTS: WIND FORECAST UNCERTAINTY AND LIMITED FEED-IN GRID CONNECTION

Mirko Ledro[1a,2,*,+], Alessandro Vicari[2,*], Gauthier Mouette[1b], Jens Jakob Sørensen[1c], Jan Martin Zepter[2], Mattia Marinelli[2]

[1a]*Ørsted Wind Power, HVDC & Grid Stabilizing Equipment, Nesa Allé 1, 2820 Gentofte, Denmark*
[1b]*Ørsted Wind Power, Short Term Trading Optimization, Nesa Allé 1, 2820 Gentofte, Denmark*
[1c]*Ørsted Wind Power, Digital Innovation, Kraftværksvej 53, 7000 Fredericia, Denmark*
[2]*Technical University of Denmark, Wind and Energy Systems, Frederiksborgvej 399, 4000 Roskilde, Denmark*
[*]*The first two co-authors contributed equally to this paper and share the main authorship*
[+]*Corresponding author, mirle@orsted.com*

Keywords: HYBRID POWER PLANT, BATTERY STORAGE, WIND FARM, WIND POWER FORECAST UNCERTAINTY, FEED-IN GRID CONNECTION

Abstract

This paper investigates the optimal operation of a wind-battery hybrid power plant. The analysis focuses on quantifying the economic difference between trading a wind power plant and a battery storage individually in the day-ahead market, or trading the wind power plant only and using the battery to minimize wind imbalance volumes. In addition, considering a limited feed-in grid connection capacity, a comparison between deterministic and stochastic optimization models to include wind forecast uncertainty is assessed, aiming at minimizing wind power curtailment. For the analysis, wind power plant and battery storage sizes are fixed at 1.3 GW and 300 MW/600 MWh, respectively. The investigation considers historical energy forecast and production data of an offshore wind power plant.

On the one hand, the economic comparison suggests that bidding both wind power plant and battery storage individually in the day-ahead market has higher profitability than using the battery to minimize imbalance volumes only. In fact, by using the battery to cover wind energy imbalances, the overall wind-battery plant profit decreases by 2.37%, even though the imbalances are reduced by 35.6%. On the other hand, including the uncertainty of wind energy production in the stochastic model, the optimized battery operations reduce the curtailed wind energy by 35%.

1 Introduction

Li-ion battery energy storage systems (BESSs) are showing their potential to enhance power system controllability when co-located with renewable production, such as wind power plants (WPPs) [1]. In fact, optimal operations of the installed BESS play a crucial role to maximize the overall wind-battery hybrid power plant (HPP) profit. Particularly, in the case of constrained feed-in grid connection, the BESS can help in minimizing wind power curtailment, too [2].

Overall, the literature has shown a marked increase in investigations about wind-battery HPP to exploit all benefits. A study based on a WPP operating in Australia's electricity market demonstrated that a wind-battery HPP can better regulate the plant dispatch [3]. In fact, by adding the BESS, the participation in both the wholesale and the ancillary service market can result in additional returns compared to standalone assets. Similarly, the authors in [4] show that from a WPP owner's perspective, a co-optimized wind-battery HPP participating in Day-Ahead (DA) and frequency containment reserve markets can increase profits and help stabilize the grid. Similar results were found in [5], where BESS integrated with a WPP increase revenue by 15.8% while reducing fluctuation penalty by 64.9%. Contrary to the benefits highlighted above, the multistage stochastic model for a wind-battery HPP described in [6] claims that the reduction of imbalances thanks to a BESS does not necessarily provide a higher economic return and can potentially increase the imbalance when optimizing for the highest revenue. Current market trends show that numerous WPP projects rely on power purchase agreements (PPAs) to reduce the risks and volatility associated with wholesale prices [7]. However, this may reduce the profitability of the WPP production as prices of PPA are generally lower than those offered in the wholesale market [8]. Consequently, by installing a BESS with the WPP, the HPP operator can potentially shift the power production to hours with higher prices. This creates a potential for analyzing the best economic operation for a co-located wind-battery system.

However, technical limitations of the grid or economic constraints cause the operator to design a so called overplanted wind-battery HPP. An overplanted HPP has a feed-in grid connection lower than the sum of the power capacities of each individual asset composing the plant. Therefore, the trading optimization of WPP and BESS assets is crucial for achieving the highest revenue stream possible, and determining how to

operate these assets to avoid unnecessary curtailment and associated penalties. This need for research is supported by Naemi et al. [3], who found that improving forecast accuracy in wind-battery HPP can lead to higher system revenue due to better regulation and precision when dispatching, along with a lower upfront investment in the BESS. Additionally, the authors in [9] show that accounting for the stochastic nature of market prices due to wind fluctuations can improve the operational scheduling of BESS, hence increasing their profit. Similar stochastic optimization technologies for wind-battery HPP are already showcased and utilized by Arenko [10]. Lastly, overplanted HPP facilities are foreseen to play an important role in an efficient green transition. For this reason, the Danish Transmission System Operator Energinet has drafted a first set of technical requirements governing co-located facilities [11].

Given all the aforementioned reasons, and inspired by Ørsted's projects, this paper intends to quantify the economic difference between trading the WPP and the BESS individually, or trading the WPP only and using the BESS to minimize the WPP imbalance. Furthermore, it compares deterministic and stochastic co-optimization of an overplanted wind-battery HPP, aiming at minimizing wind power curtailment. Historical forecast and production data of an offshore WPP are considered, together with a fixed BESS size. Consequently, the investigation aims at answering the following research questions:

1. *How much does the BESS contribute to minimize WPP forecast errors and reduce imbalance cost?*
   An economical comparison would tell if it is optimal to take advantage of the BESS to minimize the wind power forecast error, or if to bid the BESS in the wholesale market independently and allow imbalance of the WPP.
2. *How can the wind power forecast uncertainty be included in the DA trading phase when bidding the BESS in an overplanted wind-battery HPP?*
   Every wind power forecast comes with an uncertainty level which must be considered during the bidding phase. Therefore, the BESS trading should consider possible forecasted WPP production scenarios with their respective probabilities of realization. By including them in the optimization problem, the BESS is scheduled for the upcoming 24 hours, focusing on avoiding curtailment due to feed-in grid connection limitation.

The remainder of the paper is structured as follows. Chapter 2 presents the mathematical models. Chapter 3 provides an overview about the historical data and the case study. Chapter 4 highlights and discusses the main results. Chapter 5 concludes the paper and summarizes future works.

2 Methodology

This chapter presents the mathematical models to analyse the wind-battery HPP under different operational scenarios. Section 2.1 calculates the total WPP profits combining both DA market and imbalance cost. Section 2.2 formulates the optimal dispatch of the BESS to provide energy arbitrage in the DA market in case there are no grid constraints in the HPP. Section 2.3 optimizes the BESS control to minimize WPP imbalance volumes. By combining the mathematical formulation in Sections 2.1, 2.2, and 2.3, it is possible to quantify the economic difference between trading the WPP and the BESS in the DA individually, or trading the WPP only and using the BESS to minimize the WPP imbalance. Finally, Sections 2.4 and 2.5 include the deterministic and stochastic formulation, respectively, used to investigate the co-optimization of the WPP and the BESS in case grid constraints must be considered for a overplanted HPP.

2.1 WPP profit: DA market with imbalance charges

As introduced in Chapter 1, historical forecast and production data of an offshore WPP are considered. The data refer to the power forecast $P_t^{W\_DA}$ and the actual WPP production P_t^W for each settlement period t in the DA market, respectively. For the sake of simplicity, it is considered that the given forecasted energy production is coincident with the contracted energy volume in the DA market. Therefore, no additional optimization is required for the WPP, and these data can be used to calculate the overall profit and loss (PnL) of the WPP PnL^W.

First, the DA profit PnL^{W_DA} is calculated as in Eq. (1), where the forecasted WPP power production is multiplied by the DA price λ_t^{DA}, and Δt is a time factor used to convert the power forecast into contracted energy volume for each settlement period. Secondly, it is common that WPP operators, who trade expected future energy production in the DA market, are subject to imbalance pricing. Therefore, Eq. (3) calculates the imbalance charge PnL^{W_IM} due to the resulting imbalance volume $P_t^{W\_IM}$ and the imbalance price λ_t^{IM}. The imbalance price reflects all costs the system operator has in order to regulate reserve and start-up units. Finally, the overall WPP profit PnL^W is found as in Eq. (4) by combining PnL^{W_DA} and PnL^{W_IM}. It is here assumed that the WPP participates in the DA market only, disregarding potential participation in the intraday market or balancing mechanism to adjust their bids while approaching the hour of delivery. In that case, PnL^W must be modified accordingly.

$$PnL^{W\_DA} = \sum_{t \in \mathcal{T}} \lambda_t^{DA} \cdot P_t^{W\_DA} \cdot \Delta t \tag{1}$$

$$P_t^{W\_IM} = P_t^W - P_t^{W\_DA} \tag{2}$$

$$PnL^{W\_IM} = \sum_{t \in \mathcal{T}} \lambda_t^{IM} \cdot P_t^{W-IM} \cdot \Delta t \tag{3}$$

$$PnL^W = PnL^{W\_DA} + PnL^{W\_IM} \tag{4}$$

2.2 BESS profits: energy arbitrage in the DA market

The optimization model for energy arbitrage with the BESS in the DA market is reported in Eq. (5)−(13). The model allows to maximize BESS profits considering perfect foresight of DA electricity price λ_t^{DA}, but including battery constraints.

Table 1 List of sets, scalars, parameters, and variables.

Sets	
$t \in \mathcal{T}$	settlement period t in the time horizon T
$s \in \mathcal{S}$	scenario s in set of scenarios S
θ_d	set of variables of the DA model
θ_i	set of variables of the imbalance model
θ_s	set of variables of the stochastic model
Scalar	
Δt	conversion factor
E^B	BESS rated energy capacity
P^B	BESS rated power capacity
SOC_{min} / SOC_{max}	BESS state of charge lower/upper limit
η	BESS efficiency
E^W	WPP rated energy capacity
P^W	WPP rated power capacity
λ_{up} / λ_{down}	penalty factors
P^{grid}	feed-in grid connection power capacity
Parameters	
$P_t^{W\_DA}$	contracted DA WPP production for each time step t
λ_t^{DA}	DA electricity price for each time step t
$P_t^{W\_IM}$	WPP imbalance power for each time step t
π_s	probability of occurrence for each scenario s
$P_{t,s}^W$	WPP power production scenario for each time step t and scenario s
Variables	
a_t	binary variable for each time step t
Pch_t^{DA} / $Pdis_t^{DA}$	BESS DA charging / discharging power for each time step t
$Pch_{t,s}^{adj}$ / $Pdis_{t,s}^{adj}$	BESS adjustment charging / discharging power for each time step t and scenario s
Pch_t^{IM} / $Pdis_t^{IM}$	BESS imbalance charging / discharging power for each time step t
$E_t^{IM\_p}$ / $E_t^{IM\_n}$	HPP positive / negative energy imbalance after BESS correction action for each time step t
O_t^{DA}	first stage component of the stochastic model for each time step t
$O_{t,s}^{adj}$	second stage component of the stochastic for each time step t and scenario s
SOC_t	state of charge of the battery for each time step t
SOC_t^S	state of charge of the battery for each time step t, obtained via stochastic model
$SOC_{t,s}^S$	state of charge of the battery for each time step t and scenario s, obtained via stochastic model

The objective function is described in Eq. (5) and comprises λ_t^{DA} along with the discharging $Pdis_t^{DA}$ and charging power Pch_t^{DA}. The latter two terms refer to the measured power at the battery terminals, i.e., at the point of connection to the public grid, and θ_d includes the decision variables of the optimization. Eq. (6) describes the continuity of the state variable state of charge SOC_t, which is computed for each time step $t \in \mathcal{T} \setminus \{t_{init}\}$. The SOC_t at the settlement period t is calculated by summing the SOC_{t-1} in the period $t-1$ with the charging or discharging energy during period t. The efficiency η is included to account for conversion losses during charging and discharging, while the BESS energy capacity E^B is used to express the SOC_t in percentage terms. Eq. (7) restricts the SOC_t between minimum SOC_{min} and maximum SOC_{max}, while Eq. (8) and (9) limit Pch_t^{DA} and $Pdis_t^{DA}$ to the BESS power capacity P^B which is the rated power of the BESS converter. It is noted how the auxiliary binary variable a_t is introduced to ensure that charging and discharging do not take place in a settlement period t simultaneously. Finally, Eq. (10) and (11) initialize SOC_t, and Pch_t^{DA} and $Pdis_t^{DA}$ for the optimization, respectively.

$$\underset{\theta_d}{\text{Max}} \sum_{t \in \mathcal{T}} \lambda_t^{DA} \cdot \left(Pdis_t^{DA} - Pch_t^{DA}\right) \cdot \Delta t \tag{5}$$

$$\theta_d = \{Pch_t^{DA}, Pdis_t^{DA}, SOC_t, a_t\}$$

$$\text{s.t.} \quad SOC_t = SOC_{t-1} + \left(Pch_t^{DA} \cdot \eta - \frac{Pdis_t^{DA}}{\eta}\right) \cdot \frac{\Delta t}{E^B} \qquad \forall t \in \mathcal{T} \setminus \{t_{init}\} \tag{6}$$

$$SOC_{\text{min}} \leq SOC_t \leq SOC_{\text{max}} \quad \forall t \in \mathcal{T} \tag{7}$$

$$0 \leq Pch_t^{DA} \leq P^B \cdot a_t \quad \forall t \in \mathcal{T} \tag{8}$$

$$0 \leq Pdis_t^{DA} \leq P^B \cdot (1 - a_t) \quad \forall t \in \mathcal{T} \tag{9}$$

$$SOC_{t_{init}} = SOC_{t_{end}} \tag{10}$$

$$Pch_{t_{init}}^{DA} = Pdis_{t_{init}}^{DA} = 0 \tag{11}$$

$$\{Pch_t^{DA}, Pdis_t^{DA}, SOC_t\} \in \mathbb{R}_0^+ \quad \forall t \in \mathcal{T} \tag{12}$$

$$a_t \in \{0, 1\} \quad \forall t \in \mathcal{T} \tag{13}$$

2.3 Dispatching BESS to minimize WPP imbalance volumes

The optimization model to control the BESS to minimize the WPP imbalance volumes is reported in Eq. (14)−(27). In this case, the BESS is used to reduce WPP imbalances $P_t^{W\_IM}$, so only the WPP participate in the DA market.

The objective function is described in Eq. (14). The resulting imbalance volumes after the corrective action from the BESS is divided into positive $E_t^{IM\_p}$ and negative imbalance $E_t^{IM\_n}$, as in Eq. (15) and (16), respectively. Only one constraint is active per settlement period t, when the respective imbalance is present. Therefore, thanks to the different sign between $E_t^{IM\_p}$ and $E_t^{IM\_n}$ in the objective function, both imbalance terms are minimized in absolute terms. This split allows to obtain the desired optimization while keeping the model linear. θ_i includes the decision variables of the optimization. Finally, it is underlined how the imbalance price is not included in the objective function, thus the BESS schedule will not be influenced by that. In fact, imbalance cost is established by the system operator for each settlement period a month later, and it difficult to predict. It is important to highlight the strong assumption of knowing the WPP imbalance a priori, so to address the optimal schedule to minimize them. As a matter of fact, this optimization can be seen as a control model.

Eq. (17) and (18) limit Pch_t^{IM} and $Pdis_t^{IM}$ to the BESS power capacity P^B, whereas Eq. (19) and (20) limit the maximum imbalance error to WPP capacity E^W. Eq. (21)−(24) describe the continuity of the state variable SOC_t, limit the SOC_t range, and initialize SOC_t, Pch_t^{IM} and $Pdis_t^{IM}$ for the optimization, respectively, as described in Section 2.2.

$$\underset{\theta_i}{\text{Min}} \sum_{t\in\mathcal{T}} \left(E_t^{IM\_p} - E_t^{IM\_n}\right)$$

$$\theta_i = \{Pch_t^{IM}, Pdis_t^{IM}, E_t^{IM\_p}, E_t^{IM\_n}, SOC_t, a_t\} \tag{14}$$

s.t.
$$E_t^{IM\_p} = (P_t^{W\_IM} - Pch_t^{IM} - Pdis_t^{IM}) \cdot \Delta t \quad \forall t \in \mathcal{T} \quad \text{if} \quad P_t^{W\_IM} \geq 0 \tag{15}$$

$$E_t^{IM\_n} = (P_t^{W\_IM} - Pch_t^{IM} - Pdis_t^{IM}) \cdot \Delta t \quad \forall t \in \mathcal{T} \quad \text{if} \quad P_t^{W\_IM} \leq 0 \tag{16}$$

$$0 \leq Pch_t^{IM} \leq P^B \cdot a_t \quad \forall t \in \mathcal{T} \tag{17}$$

$$0 \leq Pdis_t^{IM} \leq P^B \cdot (1 - a_t) \quad \forall t \in \mathcal{T} \tag{18}$$

$$0 \leq E_t^{IM\_p} \leq E^W \quad \forall t \in \mathcal{T} \tag{19}$$

$$-E^W \leq E_t^{IM\_n} \leq 0 \quad \forall t \in \mathcal{T} \tag{20}$$

$$SOC_t = SOC_{t-1} + \left(Pch_t^{IM} \cdot \eta - \frac{Pdis_t^{IM}}{\eta}\right) \cdot \frac{\Delta t}{E^B} \quad \forall t \in \mathcal{T} \setminus \{t_{init}\} \tag{21}$$

$$SOC_{\text{min}} \leq SOC_t \leq SOC_{\text{max}} \quad \forall t \in \mathcal{T} \tag{22}$$

$$SOC_{t_{init}} = 50\% \tag{23}$$

$$Pch_{t_{init}}^{IM} = Pdis_{t_{init}}^{IM} = 0 \tag{24}$$

$$\{Pch_t^{IM}, Pdis_t^{IM}, E_t^{IM\_p}, SOC_t\} \in \mathbb{R}_0^+ \quad \forall t \in \mathcal{T} \tag{25}$$

$$E_t^{IM\_n} \in \mathbb{R}_0^- \quad \forall t \in \mathcal{T} \tag{26}$$

$$a_t \in \{0, 1\} \quad \forall t \in \mathcal{T} \tag{27}$$

2.4 DA overplanted - deterministic model

An overplanted wind-battery HPP has a feed-in grid connection capacity lower than the sum of the WPP and BESS installed power capacities. The limited grid capacity forces to discharge the BESS as function of the WPP production, or vice versa. Given that wind energy is a renewable source, it is decided to subordinate the BESS dispatch to the WPP forecast.

Therefore, the goal of the deterministic model based on a single WPP forecast is to schedule the BESS for energy arbitrage in the DA market in the case of an overplanted wind-battery HPP. The optimization model is the same as in Section 2.2, with the additional constraint in Eq. (28). This constraint ensures that the $Pdis_t^{DA}$ and $P_t^{W\_DA}$ jointly do not exceed the feed-in grid connection P^{grid} in each settlement period t. $P_t^{W\_DA}$ is the single WPP forecast, given as input to the optimization model. It is underlined that, even though this constraint is added, if the WPP production is higher than what forecasted and contracted in the DA market, the WPP or the BESS will be curtailed.

Eq. (5) – Eq. (13)

s.t. $$0 \leq Pdis_t^{DA} + P_t^{W\_DA} \leq P^{grid} \quad \forall t \in \mathcal{T} \tag{28}$$

2.5 DA overplanted - stochastic model

To account for unforeseen variation in WPP production in respect to what forecasted, the literature showed the potential of incorporating the stochastic nature of wind into the deterministic model in Section 2.4. The goal of the stochastic optimization model remains still the same, i.e., to schedule the BESS for energy arbitrage in the DA market in overplanted wind-battery HPP, but adding to the deterministic model the WPP forecast uncertainty.

Therefore, the proposed model is a two-stage stochastic model. The first stage decision is made upon a single WPP forecast, whereas the second stage is built to take into consideration a set of possible discrete scenarios, each with its probability of realization. The contracted charged and discharged BESS decisions made in the first stage need to anticipate the possible overload that could happen taking into account the second stage realizations. Consequently, the more accurate the scenario generation is, the higher the chances are to avoid BESS or WPP curtailment. The major information to build the stochastic model are taken from references [12] [13].

2.5.1 Scenario generation: Several scenario generations and reduction methods are shown in the literature. For this analysis, a randomly created scenario generation technique is considered. Scenarios $P_{t,s}^{W}$ are obtained by multiplying P_t^{W-DA} with randomly generated vectors $X_{t,s}$ which contains uniformly distributed values between x^{min} and x^{max}. Each forecast has its unique randomly generated probability of realization π_s.

$$P_{t,s}^{W} = P_t^{W-DA} \cdot X_{t,s} \quad \forall t \in \mathcal{T}, \forall s \in \mathcal{S} \tag{29}$$

$$X_{t,s} = [x_{t_{init},s}, ..., x_{t_{end},s}] \quad \forall t \in \mathcal{T}, \forall s \in \mathcal{S} \tag{30}$$

$$X_{t,s} \sim U(x^{min}, x^{max}) \tag{31}$$

$$\pi_S = [\pi_{s_{init}}, ..., \pi_{s_{end}}] \tag{32}$$

2.5.2 Stochastic model formulation: The stochastic optimization model is reported in Eq. (33)−(50). The objective function is reported in Eq. (33) and it is composed of two terms: O_t^{DA}, same objective function as for the DA overplanted deterministic model in Section 2.4 represents the first stage and it is described in Eq. (35), whereas $O_{t,s}^{adj}$ represents the second stage and it is described in Eq. (36). The BESS DA schedule is provided in the first stage of the optimization, and in the second stage an adjustment charging $Pch_{t,s}^{adj}$ and discharging BESS power $Pdis_{t,s}^{adj}$ is defined for each scenario s. $O_{t,s}^{adj}$ has a similar structure as O_t^{DA}, but includes penalty factors λ_{down} and λ_{up} to force the optimizer to schedule the BESS for energy arbitrage in the first stage as much as possible. This is necessary since the same price vector λ_t^{DA} is used for both first and second stage. Additionally, $O_{t,s}^{adj}$ includes the probability factor π_s to account for the probability of realization of each scenario s. Finally, θ_s includes all decision variables, where first stage variables only contain the t index while second stage variables also have scenario s dependency.

$$\max_{\theta_s} \sum_{t \in \mathcal{T}} O_t^{DA} + \sum_{t \in \mathcal{T}, s \in \mathcal{S}} O_{t,s}^{adj} \tag{33}$$

$$\theta_s = \{Pch_t^{DA}, Pdis_t^{DA}, Pch_{t,s}^{adj}, Pdis_{t,s}^{adj}, SOC_t^S, SOC_{t,s}^S, a_t\} \tag{34}$$

s.t.
$$O_t^{DA} = \lambda_t^{DA} \cdot \left(Pdis_t^{DA} - Pch_t^{DA}\right) \cdot \Delta_t \tag{35}$$

$$O_{t,s}^{adj} = \lambda_t^{DA} \cdot \left(Pdis_{t,s}^{adj} \cdot \lambda^{down} - Pch_{t,s}^{adj} \cdot \lambda^{up}\right) \cdot \Delta t \cdot \pi_s \tag{36}$$

$$SOC_t^S = SOC_{t-1}^S + \left(Pch_t^{DA} \cdot \eta - \frac{Pdis_t^{DA}}{\eta}\right) \cdot \frac{\Delta t}{E^B} \quad \forall t \in \mathcal{T} \setminus \{t_{init}\} \tag{37}$$

$$SOC_{\text{min}} \leq SOC_t^S \leq SOC_{\text{max}} \quad \forall t \in \mathcal{T} \tag{38}$$

$$0 \leq Pdis_t^{DA} + P_t^{W-DA} \leq P^{grid} \quad \forall t \in \mathcal{T} \tag{39}$$

$$0 \leq Pch_t^{DA} \leq P^B \cdot a_t \quad \forall t \in \mathcal{T} \tag{40}$$

$$0 \leq Pdis_t^{DA} \leq P^B \cdot (1 - a_t) \quad \forall t \in \mathcal{T} \tag{41}$$

$$SOC_{t_{init}}^S = SOC_{t_{end}}^S \tag{42}$$

$$Pch_0^{DA} = Pdis_0^{DA} = 0 \tag{43}$$

$$SOC_{t,s}^S = SOC_{t-1,s}^S + \left((Pch_t^{DA} + Pch_{t,s}^{adj}) \cdot \eta - \frac{Pdis_t^{DA} + Pdis_{t,s}^{adj}}{\eta}\right) \cdot \frac{\Delta t}{E^B} \quad \forall t \in \mathcal{T} \setminus \{t_{init}\}, \forall s \in \mathcal{S} \tag{44}$$

$$SOC_{\text{min}} \leq SOC_{t,s}^S \leq SOC_{\text{max}} \quad \forall t \in \mathcal{T} \quad \forall s \in \mathcal{S} \tag{45}$$

$$0 \leq Pch_t^{DA} + Pch_{t,s}^{adj} \leq P^B \quad \forall t \in \mathcal{T} \quad \forall s \in \mathcal{S} \tag{46}$$

$$0 \leq Pdis_t^{DA} + Pdis_{t,s}^{adj} \leq P^B \quad \forall t \in \mathcal{T} \quad \forall s \in \mathcal{S} \tag{47}$$

$$0 \leq P_{t,s}^{W} + (Pdis_t^{DA} + Pdis_{t,s}^{adj} - Pch_t^{DA} - Pch_{t,s}^{adj}) \leq P^{grid} \quad \forall t \in \mathcal{T}, \forall s \in \mathcal{S} \tag{48}$$

$$SOC_{t_{init},s}^S = SOC_{t_{end},s}^S \quad \forall s \in \mathcal{S} \tag{49}$$

$$Pch_{t_{init},s}^{adj} = Pdis_{t_{init},s}^{adj} = 0 \quad \forall s \in \mathcal{S} \tag{50}$$

Eq. (37)−(50) contain all constraints of the stochastic model. Eq. (37)−(43) refer to the first stage and they have been described in Section 2.2 and 2.4, whereas Eq. (44)−(50) refer to the second stage. They have the same structure as for the first stage, but including variables referred to the second stage as well as the scenario dependency. Finally, Eq. (48) ensures the overall wind-battery HPP does not exceed the feed-in grid connection capacity.

3 Historical data and case study

Section 3.1 reports the imbalance cost analysis due to the mismatch between WPP contracted volumes in the DA market and realized production, whereas Section 3.2 describes the case studies.

3.1 Historical data: imbalance cost analysis

Ørsted Wind Power provided historical half-hourly energy forecast and production data of an offshore WPP. Since the data are used for DA trading, the selected forecast data for day d are updated based on the last available expected production at 9:00am on day d-1. Additionally, these data were received as normalized format in respect to the WPP capacity, however the WPP name and capacity are unknown. Therefore, they are scaled and applied to a 1.3 GW WPP, hypothetically located in the UK. The data span from January 2020 to December 2022.

Wind farm operators, who trade expected future energy production in the DA market, are subject to imbalance pricing. Therefore, the analysis calculates the energy imbalance volumes due to WPP forecast errors. Considering that a dual imbalance price scheme is in force in the UK, four possible cases $c1$-$c4$ are reported in Table 2 [14].

Table 2 Imbalance scenarios

Case	Wind farm	System	Frequency share (%)	Average imbalance (MWh)
c1	Long	Long	15.17	48.75
c2	Long	Short	18.03	58.95
c3	Short	Long	35.88	55.78
c4	Short	Short	29.72	43.52

The cases differ based on the imbalance of the contracted WPP volume and the overall transmission system imbalance. On the one hand, $c1$ and $c2$ refer to WPP who is long and subject to system sell price (SSP) – the WPP needs to sell the surplus production at SSP, whereas $c3$ and $c4$ to WPP who is short and subject to system buy price (SBP) – the WPP needs to buy the deficit production at price SBP. In the UK, there is a single price calculation, so SSP and SBP are equal in each settlement period t, and here referred to as imbalance price λ_t^{IM}. On the other hand, $c1$ and $c3$ refer to when the overall transmission system is long, and the imbalance price λ_t^{IM} is higher than the DA price λ_t^{DA}, whereas $c2$ and $c4$ refer to a short transmission system and λ_t^{IM} lower than the λ_t^{DA}. Therefore, an imbalance of the contracted WPP volume in $c1$ or $c4$ represents a profit-making event, while the same imbalance in $c2$ or $c3$ represents a loss-making event [15].

The imbalance analysis applied to the available historical data give the frequency share of each scenario and the average imbalance volume in Table 2. The analysis shows that $c1$ and $c4$ represent about 45% of the frequency share collectively, while $c2$ and $c3$ account for the complementary 55%. This indicates that an imbalance volume would benefit the WPP operator for 45% of the time roughly, generating higher revenues compared to a perfect foresight case. Conversely, an imbalance volume would result in a cost for the WPP operator for the complementary 55% of the time.

3.2 Case study

The case study focuses on the three representative days data from March 15 to March 17, 2021. The WPP forecast and production data, together with DA and imbalance prices are displayed in Fig 1. The data are provided with 30 min granularity, which corresponds to the time duration of each settlement period t of the UK DA afternoon auction. In these days, the WPP forecast and production is close to its nominal installed capacity, as well as very low. Additionally, a sharp ramp up in power production is expected around hour 38, but the measured power shows a clear phase shift between forecast and production. This event allows to showcase the potential of using the BESS to cover for WPP imbalance volumes. Therefore, P^W and E^W are 1.3 GW and 1.3 GWh, respectively.

Regarding the BESS, its size is considered fixed a priori. The installed energy capacity E^B is 600 MWh, whereas the installed rated power of the converter P^B is 300 MW. Additionally, by considering an overall round trip efficiency of 85%, and assuming same losses during charging and discharging processes, the resulting one-way efficiency η is 92.25%. The BESS is allowed to operate in the whole SOC range, therefore SOC_{min} and SOC_{max} are 0 and 1, respectively.

Considering the stochastic analysis, the parameters are set arbitrarily as follows. The penalty factors λ^{down} and λ^{up} are fixed at 0.8 and 1.2, whereas x^{min} and x^{max} are 0.9 and 1.1. Assuming a total number of three scenarios $s1$, $s2$, and $s3$, the probability of realization for each scenario π_1, π_2, and π_3 is 0.32, 0.4, and 0.28, respectively. The generated scenarios are reported in Fig. 2.

Finally, the feed-in grid connection capacity P^{grid} is fixed at 1.3 GW. However, P^{grid} is increased in steps of 0.5 GW in the sensitivity analysis.

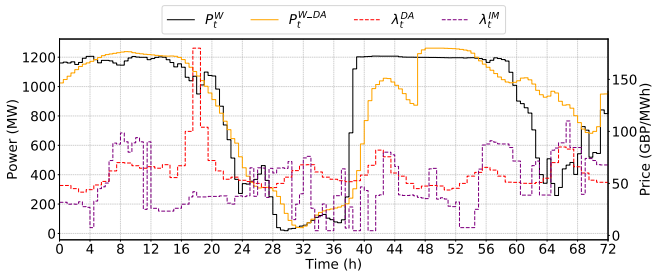

Fig. 1 Three days horizon: WPP forecast and production, DA and imbalance price

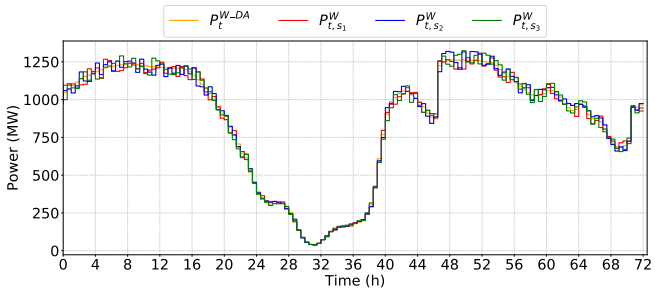

Fig. 2. Generated scenarios of WPP production

4 Results and discussion

This chapter reports and discusses the obtained results by combining the methodology in Chapter 2 to the data and case study in Chapter 3. On the one hand, Section 4.1 answers the first research question by quantifying the economic difference between trading the WPP and the BESS individually, or trading the WPP only and using the BESS to minimize the WPP imbalance. On the other hand, Section 4.2 answers to the second research question by comparing deterministic and stochastic co-optimization of an overplanted wind-battery HPP, and including a sensitivity analysis about the feed-in grid connection capacity applied to the stochastic optimization. The results are obtained in Python using Gurobi solver package.

4.1 Optimal operation of wind-battery HPP

This section evaluates if the wind-battery HPP would benefit from trading both WPP and the BESS individually in the DA and going into imbalance with the WPP, or if it is more economically favorable to use the BESS to minimize the WPP imbalance volumes. First, results from the BESS participating in DA market are shown, followed by the outcome of operating the BESS to minimize the WPP imbalance volume. Finally, a comparison between the two operational scenarios is discussed.

4.1.1 BESS traded in the DA market: The result of providing energy arbitrage with the BESS in the DA market is reported in Fig. 3, where the SOC_t is plotted together with the electricity price λ_t^{DA}. SOC_t increases when the price is relatively

low due to a lower cost for charging the BESS, whereas the SOC_t decreases when the price is relatively high since the model generates higher revenues when discharging the BESS.

The overall wind-battery HPP production is shown in Fig. 4. It represents the expected HPP power production (dashed green line), which is obtained by combining the WPP contracted DA generation (orange line), BESS discharging power (blue line), and BESS charging power (pink line), with the BESS following the generator sign convention. The areas below the WPP and BESS power profiles represent the contracted energy volume in the 30 min DA market auction. Overall, the HPP injection into the grid is lower than the WPP production if the BESS charges, otherwise greater than the WPP production if the BESS discharges. The measured HPP production (black line) is obtained by summing the measured WPP generation to the BESS traded profile. The impact of the wind power production uncertainty is clearly visible. For example, at around hour 38, the expected HPP power production is zero due to low wind power production and the BESS charging. However, the measured HPP production is 800 MW.

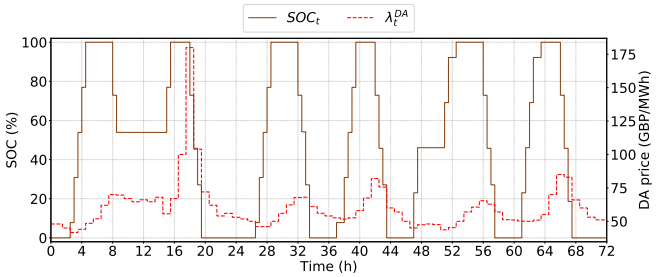

Fig. 3. SOC profile and DA price

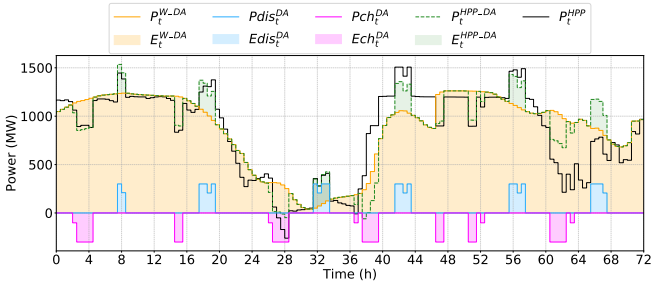

Fig. 4. HPP overview: BESS traded in the DA market

4.1.2 BESS for minimizing WPP imbalances: The result of controlling the BESS to minimize WPP imbalance volumes is reported in Fig. 5, where the SOC_t (brown line) is plotted together with the WPP imbalance volumes before (green line) and after (red line) BESS correction action. Additionally, Fig. 6 shows the overall wind-battery HPP production, highlighting the difference between expected and measured HPP production. Given the chosen BESS size, imbalance volumes are visibly reduced in the first half of the simulation, since the BESS can cover them. However, if the imbalances are towards a direction repetitively (often negative, or often positive) or of too high magnitude, the BESS cannot cover them as shown in the second half of the simulation. Additionally, it is observed how the optimization could even increase the WPP imbalances in certain settlement periods, when the optimization prefers to get ready for future corrective actions. Overall, the results show the potential inefficiency of covering the DA imbalance volumes of a 1.3 GW WPP with the use of a 300 MW/600 MWh BESS.

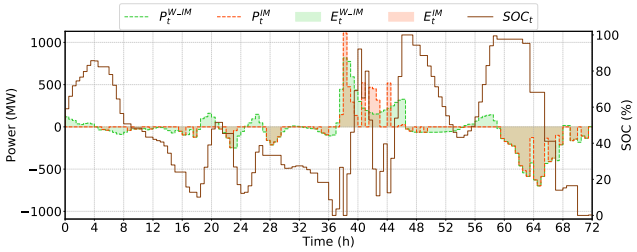

Fig. 5. SOC profile and WPP imbalance volumes

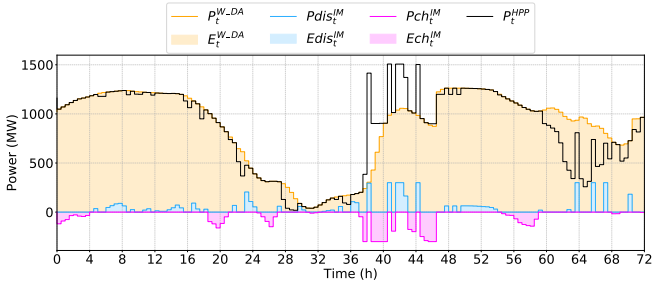

Fig. 6. HPP overview: BESS minimizes imbalances

4.1.3 Comparison between BESS in the DA market and for minimizing WPP imbalances: To address the first research question, Table 3 collects results for the overall HPP, comparing the outcome from bidding the BESS in the DA market or the BESS for covering WPP imbalance volumes. Results are gathered for the selected three days, as well as for a week and a month.

It is observed that the PnL for the HPP is higher if the BESS is traded in the DA market, instead of using the BESS to cover for WPP imbalances. For example, considering the three-day time horizon, the HPP PnL decreases by 2.37%, even though the WPP imbalances are reduced by 35.6%. This is attributed to the BESS, which generates higher revenue when participating in the DA market, compared to the benefits it could provide by reducing the imbalance error. In fact, considering Eq. (14), it is clear that the optimization aims to minimize the energy imbalance without taking into consideration any imbalance cost, since unknown and difficult to predict. Therefore, the overall WPP imbalance volume is decreased, but still present in settlement periods t when the imbalance cost is relatively high, as seen in Fig. 7. Additionally, an imbalanced condition does not necessarily mean that it will become a cost for the system, as described in Table 2. Similar results are observed for one-week and one-month analyses, without any clear trend to be highlighted. For the one-week and one-month horizons, the PnL decreases by 7.21% and 5.85% against a reduced imbalance

Table 3 Comparison of the wind-battery HPP operations

Time horizon	WPP and BESS in DA market		WPP in DA market, BESS for imbalances		ΔPnL		ΔImbalance	
	PnL (kGBP)	Imbalance (MWh)	PnL (kGBP)	Imbalance (MWh)	(kGBP)	(%)	(MWh)	(%)
Three days	3,670	10,111	3,583	6,511	-87	-2.37	-3,600	-35.6
One week	7,734	15,303	7,176	11,255	-557	-7.21	-4,048	-26.5
One month	33,013	81,957	31,082	58,787	-1,930	-5.85	-23,170	-28.3

volume of 26.5% and 28.3%, respectively. In conclusion, the economical comparison suggests that bidding the BESS in the DA market has higher profitability than using it for minimizing the WPP imbalance volumes.

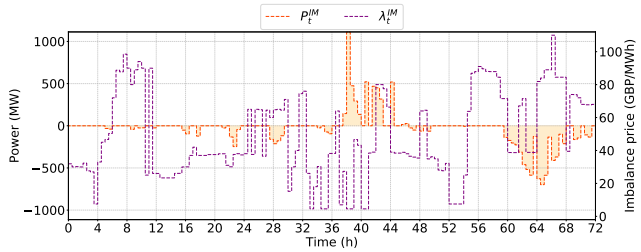

Fig. 7. Imbalance after BESS correction and imbalance price

4.2 *Optimal operation of an overplanted wind-battery HPP*

This section evaluates the optimal operation for the overplanted wind-battery HPP, where a co-optimization is required to trade the BESS due to the limited feed-in grid connection, which is fixed at the WPP installed capacity initially. First, results from the deterministic DA trading model are shown, followed by the outcome from the stochastic DA trading model, which includes WPP forecast uncertainty. Finally, a comparison between deterministic and stochastic optimization results is discussed, including a sensitivity analysis on the feed-in grid connection capacity applied to the stochastic model. Given the results from Section 4.1, the BESS is dispatched in the DA market, and not for minimizing WPP imbalance volumes.

4.2.1 Deterministic DA trading: The result of co-optimizing the BESS as function of a deterministic WPP forecast in overplanted HPP is reported in Fig. 8. Differently from Section 4.1.1, the feed-in grid connection capacity at 1.3 GW limits the BESS trading. Consequently, the BESS discharging power (blue line) could appear intermittent and below the installed BESS rated power throughout the three-day analysis. This is due to WPP forecast (orange line) being close to its rated capacity in some settlement periods, so almost reaching the feed-in grid connection limit. Observing the expected HPP production (green line), it is forecasted that the HPP would exceed the grid connection capacity, and the optimization needs to limit the BESS discharging power to avoid exceeding the feed-in limit. However, the real HPP production (black line) shows the impact of the wind forecast uncertainty, requiring curtailment actions to avoid being above the feed-in grid connection.

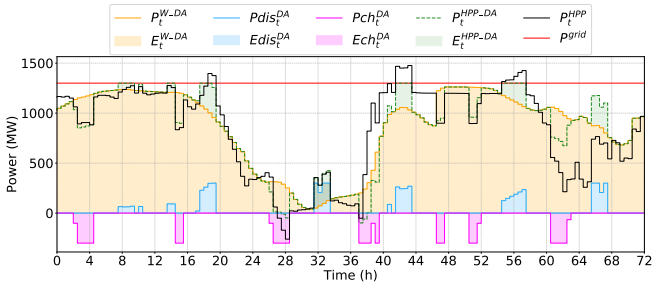

Fig. 8. Overplanted HPP overview: deterministic model

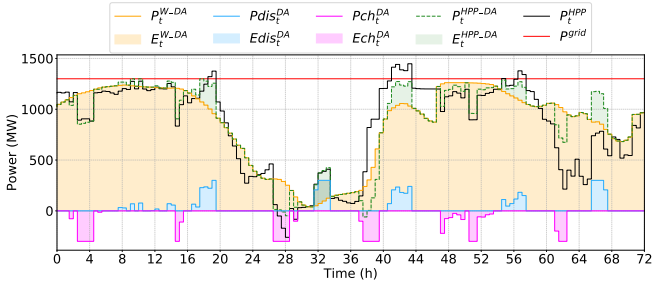

Fig. 9. Overplanted HPP overview: stochastic model

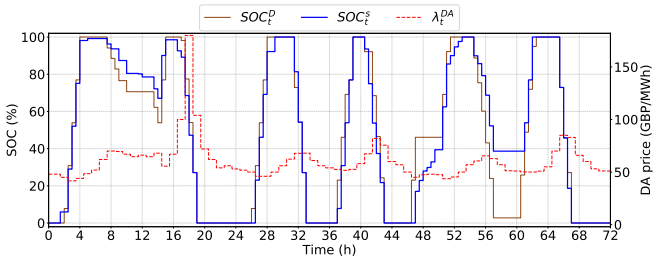

Fig. 10. SOC profiles and DA price

4.2.2 Stochastic DA trading: The results of co-optimizing the BESS considering the influence of the stochastic behaviour of the WPP in overplanted HPP is reported in Fig. 9. The expected HPP production (dashed green line) appears to be clearly below the grid connection capacity throughout the three-day analysis, thus allowing possible WPP overproduction in respect to the contracted volume. This is possible thanks to an adjusted BESS discharge power (blue line) in respect to the deterministic analysis. More specifically, Fig. 10 shows SOC_t of the BESS for both deterministic (SOC_t^D, brown line) and stochastic (SOC_t^S, blue line) model. SOC_t^S for the stochastic has smoother steps in respect to SOC_t^D for the deterministic, which is translated

in the BESS dispatched power profile described above. Finally, the real HPP production (black line in Fig. 9) shows the impact of the wind forecast uncertainty, being still necessary to curtail wind power production to avoid being above the feed-in grid connection.

4.2.3 Comparison between deterministic and stochastic models: Considering the three-day time horizon, the main differences between the deterministic and stochastic models are reported in Table 4. The data in the table refers to the resulting HPP production (black line in Fig. 8 and 9).

The injected energy into the grid from the HPP does not differ significantly. In fact, the WPP is the asset generating the most, thus the impact of BESS operation is modest. Nonetheless, the adjustment in BESS discharged power with the stochastic model reduces the exceeding energy due to grid constraint of 35% in respect to the deterministic case. Additionally, it reduces the amount of time when curtailment is necessary too. This improvement is possible thanks to the higher margin for unforeseen WPP power production of the stochastic model. From the economical perspective, the revenues of the BESS from the DA market for the considered three days analysis with the deterministic model are higher than with the stochastic approach, which shows a 6.55% reduction in profit. However, even though the PnL of the BESS worsened, the stochastic model includes other WPP realizations than the given single WPP forecast, thus the contracted DA trading is more aware of potential WPP deviations.

Table 4 Comparison of overplanted HPP operations

Optimization model	Deterministic	Stochastic
Delivered energy (MWh)	64,369	64,086
Overproduction (hh)	12	10
Exceeding energy (MWh)	600	394
BESS PnL from DA (kGBP)	85.35	79.76

4.2.4 Sensitivity analysis of feed-in grid connection capacity: The analysis above showed the results when considering a feed-in grid connection capacity of 1.3 GW, which is equal to the WPP installed capacity P^W. Therefore, a sensitivity analysis is reported in Table 5, where the grid connection capacity is increased from 1.3 GW up to 1.6 GW with 0.5 GW steps. Overall, the total PnL increases with the grid connection capacity, ending up converging at around 14% PnL increased for a grid capacity of 1.45 GW or above. The improvement in PnL is justified by the freedom for the BESS to discharge in those settlement periods where higher prices are seen, resulting in a higher profit for the HPP by maintaining fairly constant the delivered energy. Additionally, the exceeding energy production decreases with a higher grid connection, being zero already with 1.55 GW connection capacity, 0.5 GW lower than the sum of the WPP and the BESS. In conclusion, increasing the feed-in grid connection capacity allows more freedom of scheduling the BESS. However, an economic comparison including the grid connection cost should be carried to justify and weigh up the overall profit.

5 Conclusion

The paper investigated the optimal operation of a wind-battery HPP. Firstly, the analysis focused on quantifying the economic difference between trading a 1.3 GW WPP and a 300 MW/600 MWh BESS individually in the DA market, or trading the WPP only and using the BESS to minimize WPP imbalance volumes. Lastly, a limited feed-in grid connection capacity is considered, and a comparison between deterministic and stochastic optimization models to include WPP forecast uncertainty is assessed, aiming at minimizing the WPP curtailment.

On the one hand, the economical comparison suggests that bidding the BESS in the DA market has higher profitability than using it for minimizing the WPP imbalance volumes. For the considered three days analysis, the overall HPP profit decreases by 2.37%, even though the WPP imbalances are reduced by 35.6%. Similar patterns are observed for a longer time horizon. On the other hand, considering a grid connection of 1.3 GW, the BESS operations in the wind-battery HPP are subject to the forecasted WPP energy production. By including the uncertainty of wind production in the stochastic model in the three days analysis, the optimized BESS operations reduce the curtailed wind energy of 35% in respect to the deterministic approach. However, from the economical perspective, BESS revenues from the DA market with the stochastic model are 6.55% lower than with a deterministic approach.

Future investigation should focus on the overplanted wind-battery analysis mainly. First, since the feed-in grid connection is expressed in power terms, a WPP power profile with higher resolution than the available 30 min would improve the wind power curtailment detection. Second, a more advanced scenario generation approach could potentially increase the reliability of the stochastic model. By improving the scenario generations, evaluating the stochastic model via value of stochastic solution and other metrics are of main importance. Finally, uncertainty around DA prices should be included too.

Table 5 Sensitivity analysis: feed-in grid connection capacity

Feed-in grid connection (MW)	1.30	1.35	1.40	1.45	1.50	1.55	1.6
Delivered energy (MWh)	64,086	64,321	64,384	64,384	64,384	64,384	64,384
Overproduction (hh)	10	8	6	5	3	0	0
Exceeding energy (MWh)	394	299	227	129	10.5	0	0
BESS PnL DA (kGBP)	79.76	86.28	89.85	91.09	91.24	91.29	91.29
BESS PnL increase (%)	-	8.18	12.7	14.2	14.4	14.4	14.4

6 CRediT authorship contribution statement

Mirko Ledro: Conceptualization, Formal analysis, Funding acquisition, Investigation, Methodology, Project administration, Supervision, Writing - original draft, Writing - review & editing. **Alessandro Vicari**: Conceptualization, Data curation, Formal analysis, Investigation, Methodology, Visualization, Writing - original draft, Writing - review & editing. **Gauthier Mouette**: Conceptualization, Supervision. **Jens Jakob Sørensen**: Conceptualization, Supervision. **Jan Martin Zepter**: Conceptualization, Methodology, Project administration, Supervision, Writing - review & editing. **Mattia Marinelli**: Conceptualization, Funding acquisition, Supervision, Writing - review & editing.

All authors have read and agreed to the published version of the manuscript. The first two co-authors contributed equally to this paper and share the main authorship.

7 Acknowledgements

The authors thank Edoardo Simioni, former Head of the Short Term Trading Optimization department at Ørsted Wind Power, for all the given input to shape this research project.

8 Conflicts of interest

The authors declare no conflict of interest.

9 Funding

This work has received funding from the OBELICS (Offshore wind-Battery Energy Li-Ion Control Scheme) Industrial PhD project at Ørsted Wind Power A/S.

References

[1]M. Ledro, L. Calearo, J. M. Zepter, T. Gabderakhmanova, and M. Marinelli, "Influence of realistic EV fleet response with power and energy controllers in an EV-wind virtual power plant," *Sustainable Energy, Grids and Networks*, vol. 31, p. 100 704, Sep. 2022, ISSN: 2352-4677. DOI: 10.1016/J.SEGAN.2022.100704.

[2]D. Villanueva, A. E. Feijóo, and N. D. Bokde, "A Strategy for Power Generation Optimization in a Hybrid Wind-BESS Power Plant," in *E3S Web of Conferences*, vol. 122, EDP Sciences, Oct. 2019. DOI: 10.1051/e3sconf/201912204004.

[3]M. Naemi, D. Davis, and M. J. Brear, "Optimisation and analysis of battery storage integrated into a wind power plant participating in a wholesale electricity market with energy and ancillary services," *Journal of Cleaner Production*, vol. 373, p. 133 909, Nov. 2022, ISSN: 0959-6526. DOI: 10.1016/J.JCLEPRO.2022.133909.

[4]Peng H., Guangya Y., Peter E., and Arne H., "Cooperation of Offshore Wind Farm with Battery Storage in Multiple Electricity Markets," in *2018 53rd International Universities Power Engineering Conference (UPEC 2018)*, Glasgow, UK, Sep. 2018, ISBN: 9781538629109.

[5]X. Xu, W. Hu, D. Cao, *et al.*, "Economic feasibility of a wind-battery system in the electricity market with the fluctuation penalty," *Journal of Cleaner Production*, vol. 271, Oct. 2020, ISSN: 09596526. DOI: 10.1016/j.jclepro.2020.122513.

[6]F. J. Heredia, M. D. Cuadrado, and C. Corchero, "On optimal participation in the electricity markets of wind power plants with battery energy storage systems," *Computers & Operations Research*, vol. 96, pp. 316–329, Aug. 2018, ISSN: 0305-0548. DOI: 10.1016/J.COR.2018.03.004.

[7]A. Loukatou, P. Johnson, S. Howell, and P. Duck, "Optimal valuation of wind energy projects co-located with battery storage," *Applied Energy*, vol. 283, Feb. 2021, ISSN: 03062619. DOI: 10.1016/j.apenergy.2020.116247.

[8]I. Staffell and M. Rustomji, "Maximising the value of electricity storage," *Journal of Energy Storage*, vol. 8, pp. 212–225, Nov. 2016, ISSN: 2352-152X. DOI: 10.1016/J.EST.2016.08.010.

[9]H. Akhavan-Hejazi and H. Mohsenian-Rad, "Optimal operation of independent storage systems in energy and reserve markets with high wind penetration," *IEEE Transactions on Smart Grid*, vol. 5, no. 2, pp. 1088–1097, Mar. 2014, ISSN: 19493053. DOI: 10.1109/TSG.2013.2273800.

[10]Andy Colthorpe, *'Complex' optimisation of co-located wind and battery storage 'creates blueprint for portfolio management'*, Oct. 2023. [Online]. Available: https://www.energy-storage.news/complex-optimisation-of-co-located-wind-and-battery-storage-creates-blueprint-for-portfolio-management-says-uks-arenko/.

[11]Energinet, *FORVENTEDE TEKNISKE KRAV FOR SAMPLACEREDE OG/ELLER OVERPLANTEDE ANLÆG TILSLUTTET TRANSMISSIONSSYSTEMET*, 2024. [Online]. Available: https://energinet.dk/om-os/arrangementer/tekniske-krav-for-samplacerede-og-eller-overplantede-anlaeg-210324/.

[12]Birge, John R., and Louveaux F., *Introduction to Stochastic Programming*. Springer, 1997, pp. 1–150.

[13]J. M. Zepter, A. Lüth, P. Crespo del Granado, and R. Egging, "Prosumer integration in wholesale electricity markets: Synergies of peer-to-peer trade and residential storage," *Energy and Buildings*, vol. 184, pp. 163–176, Feb. 2019, ISSN: 03787788. DOI: 10.1016/j.enbuild.2018.12.003.

[14]Elexon, *Imbalance Pricing*. [Online]. Available: https://www.elexon.co.uk/settlement/imbalance-pricing/.

[15]Elexon, *Imbalance Pricing Guidance*, Jun. 2020. [Online]. Available: https://bscdocs.elexon.co.uk/guidance-notes/imbalance-pricing-guidance.